

# Computation Rate Maximization in STAR-RIS aided Wireless Powered Mobile Edge Computing Networks with NOMA

MohammadHossein Alishahi\*, Paul Fortier\*, Ming Zeng\*, Fang Fang†

\*Department of Electric and Computer Engineering, Laval University, Quebec City, Canada

†Department of Electrical and Computer Engineering, Western University, London, Canada

Email: mohammadhossein.alishahi.1@ulaval.ca; paul.fortier@gel.ulaval.ca; ming.zeng@gel.ulaval.ca; fang.fang@uwo.ca

**Abstract**—This paper integrates mobile edge computing (MEC), non-orthogonal multiple access (NOMA), simultaneous transmitting and reflecting reconfigurable intelligent surface (STAR-RIS), and wireless power transfer (WPT) to enhance the computational capabilities of Internet-of-Things (IoT) devices. A joint resource allocation problem is formulated to maximize the overall computation rate of two clusters of IoT devices. To address the non-convexity of the problem, we leverage semi-definite relaxation and bisection algorithms to obtain optimized amplitude and phase shifts of STAR-RIS, time, and power allocation for energy transfer and offloading. Numerical results show the necessity of phase shift optimization in STAR-RIS and the superiority of NOMA over its orthogonal multiple access counterpart in terms of total offloaded data size.

## I. INTRODUCTION

The field of Internet-of-Things (IoT) has experienced remarkable expansion, characterized by the interconnection of billions of devices that serve diverse applications, including but not limited to intelligent virtual assistants, autonomous vehicles, and predictive healthcare [1]. Although the proliferation of IoT holds the potential for transformative advantages, it concurrently introduces significant obstacles in the form of limited energy resources and constrained computing and communication capabilities for wireless networks [2], [3]. These constraints have spurred the emergence of innovative technologies such as wireless power transfer (WPT), mobile edge computing (MEC), and non-orthogonal multiple access (NOMA), which offer a promising approach to tackle these challenges and empower resource-constrained IoT devices to operate with enhanced effectiveness and efficiency [4], [5].

Nonetheless, the relentless expansion in the density and coverage of next-generation communication systems has given rise to challenges characterized by the increasing intricacy and diversity of communication environments, often exacerbated by geographical restrictions [1]. Consequently, radio waves may either fail to be received or arrive under sub-optimal conditions in terms of signal quality. In response to these issues, a novel technology known as reconfigurable intelligent surfaces

(RIS) has emerged, demonstrating its capability of creating a controllable wireless propagation environment [6]. However, note that standard RIS only reflects the incident signals, and, thus, can serve only the users located on the same plane of itself. To allow RIS to aid the users on the opposite side as well, simultaneous transmitting and reflecting reconfigurable intelligent surface (STAR-RIS) has been proposed, where each individual element within STAR-RIS has the capability to simultaneously transmit and reflect signals. Recently, STAR-RIS has been integrated with NOMA or MEC to improve the system's energy efficiency and computation rate performance under geographical restrictions [7]–[9].

Under this context, this paper proposes a STAR-RIS aided WPT MEC network with NOMA to maximize the total computation rate of two clusters of IoT devices. The formulated problem requires to jointly optimize the time and power resources for energy harvesting and information transmission as well as the STAR-RIS phase shifts and amplitudes. To the best of our knowledge, this is the first work that integrates WPT, MEC, STAR-RIS, and NOMA for IoT. Briefly, the contributions of this paper can be summarized as follows:

- We propose a STAR-RIS aided WPT MEC network with NOMA to support the computational offloading of IoT devices.
- We formulate a computation rate maximization problem, which is constrained by the overall delay, total energy harvested from the access point (AP), and the amplitudes and phase shifts of transmission and reflection sides of the STAR-RIS. Semi-definite relaxation (SDR) is first employed to handle the RIS amplitude and phase shift optimization during both energy harvesting and offloading. On this basis, the bisection method is proposed to optimize the power and time for energy transfer and uplink transmission.
- Numerical results confirm that the proposed approach can significantly improve the total computation rate compared with the benchmark schemes. Additionally, the NOMA-

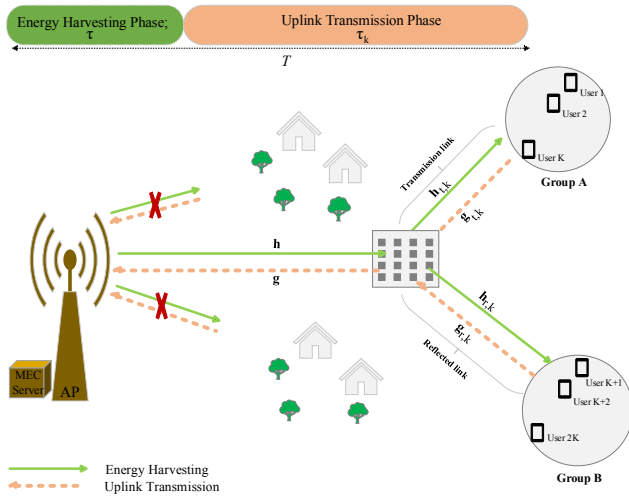


Figure 1: STAR-RIS aided wireless-powered MEC network with NOMA.

based scheme can remarkably achieve a higher computational rate than its orthogonal multiple access (OMA)-based counterpart under all considered scenarios.

## II. SYSTEM MODEL AND PROBLEM FORMULATION

### A. System Model

Figure 1 illustrates a WPT-empowered MEC system, which includes a single antenna AP and two  $K$  user clusters indexed by  $\mathcal{K}_1 = \{1, \dots, K\}$  and  $\mathcal{K}_2 = \{K+1, \dots, 2K\}$ . It is assumed that no direct link exists between the AP and users due to obstructions. A STAR-RIS with  $N$  elements, indexed by  $\mathcal{N} = \{1, \dots, N\}$ , is deployed to assist the energy transfer and communications between the AP and users in energy-splitting mode, that is, each element splits the energy of the incident signal into the transmitted and reflected parts [7].

In the considered system, the AP first broadcasts energy to the users, and then, the users utilize the harvested energy to offload their computational intensive tasks to the MEC server located at the AP [10]. The energy transfer and uplink channels between the AP and STAR-RIS are respectively denoted by  $\mathbf{h} \in \mathbb{C}^{N \times 1}$  and  $\mathbf{g}^H \in \mathbb{C}^{1 \times N}$ . Furthermore,  $\mathbf{h}_{t,k}^H \in \mathbb{C}^{1 \times N}$  and  $\mathbf{g}_{t,k}^H \in \mathbb{C}^{N \times 1}$  represent the transmission channels between the STAR-RIS and user  $k$ ,  $k \in \mathcal{K}_1$ , whereas  $\mathbf{h}_{r,k}^H \in \mathbb{C}^{1 \times N}$  and  $\mathbf{g}_{r,k}^H \in \mathbb{C}^{N \times 1}$  denote the reflection channels for user  $k$ ,  $k \in \mathcal{K}_2$ . Note that  $\mathbf{h}_{t,k}^H$  and  $\mathbf{g}_{t,k}^H$  are zero  $\forall k \in \mathcal{K}_2$ , while  $\mathbf{h}_{r,k}^H$  and  $\mathbf{g}_{r,k}^H$  are zero  $\forall k \in \mathcal{K}_1$ . The variance of the additive white Gaussian noise at the AP is  $\sigma^2$ .

The transmission and reflection vectors of the STAR-RIS for both phases can be defined as

$$\mathbf{v}_{\mathcal{Y}}^{\mathcal{X}} = \left( \sqrt{\alpha_{\mathcal{Y},1}^{\mathcal{X}}} e^{j\phi_{\mathcal{Y},1}^{\mathcal{X}}}, \dots, \sqrt{\alpha_{\mathcal{Y},N}^{\mathcal{X}}} e^{j\phi_{\mathcal{Y},N}^{\mathcal{X}}} \right)^{\top}, \quad (1)$$

where  $\mathcal{X} = \{t, r\}$  is used to indicate either the reflected or the transmitted signal is considered, while  $\mathcal{Y} = \{e, u\}$  represents either the energy transfer phase or the uplink transmission one. Besides,  $\alpha_{\mathcal{Y},n}^{\mathcal{X}} \in [0, 1]$  and  $\phi_{\mathcal{Y},n}^{\mathcal{X}} \in [0, 2\pi)$ ,  $\forall n \in \mathcal{N}$  denote respectively each element's amplitude and phase shift in transmission or reflection for both phases. According to the law of energy conservation [7], [11], these amplitudes are limited by

$$\alpha_{\mathcal{Y},n}^t + \alpha_{\mathcal{Y},n}^r = 1, \quad \mathcal{Y} = \{e, u\}, \forall n \in \mathcal{N}. \quad (2)$$

Given the above explanation and definition, now let us look at the two phases in details.

1) *Energy Transfer*: Each user in time  $\tau$  linearly harvests energy from the AP with the aid of STAR-RIS, and the corresponding harvested energy is given by [4]

$$E_k = \eta P \tau h_{e,k}, \quad (3)$$

where  $P$  is the transmission power at the AP, while  $\eta \in (0, 1)$  stands for the energy conversion efficiency factor at the user side. Besides,  $h_{e,k} = |\mathbf{h}_{t,k}^H \text{diag}(\mathbf{v}_e^t) \mathbf{h}|^2 + |\mathbf{h}_{r,k}^H \text{diag}(\mathbf{v}_e^r) \mathbf{h}|^2$  denotes the channel response in the energy transfer phase, respectively. Note that for any user in the two clusters, only one term on the right side of  $h_{e,k}$  is active, while the other one is just zero.

2) *Task Offloading Phase*: Once energy harvesting is finished, the users will start to offload their data to the MEC server located at the AP using NOMA simultaneously. At the AP, successive interference cancellation (SIC) is employed by decoding the users with better channel gains earlier, like [12]. Without loss of generality, it is assumed that the users are arranged in a descending order based on the channel gains. Denote the transmission power and offloading time for user  $k$  as  $P_k$  and  $\tau_k$ , respectively. The corresponding energy consumption is given by [13]

$$E_{k,off} = P_k \tau_k, \quad (4)$$

while the total offloaded bits at user  $k$  can be expressed as [10], [12]

$$L_k(\tau_k, P_k, h_{u,k}) = B \tau_k \log_2 \left( 1 + \frac{P_k h_{u,k}}{\sum_{m \notin \mathcal{Q}, m > k} P_m h_{u,m} + \sum_{n \in \mathcal{Q}} P_n h_{u,n} + \sigma^2} \right), \quad (5)$$

where

$$\mathcal{Q} \in \begin{cases} \mathcal{K}_2 & \text{if } k \in \mathcal{K}_1 \\ \mathcal{K}_1 & \text{if } k \in \mathcal{K}_2, \end{cases} \quad (6)$$

Besides,  $B$  denotes the total bandwidth, while  $h_{u,k} = |\mathbf{g}^H \text{diag}(\mathbf{v}_u^t) \mathbf{g}_{t,k}|^2 + |\mathbf{g}^H \text{diag}(\mathbf{v}_u^r) \mathbf{g}_{r,k}|^2$  is the uplink transmission channel gain.  $\sum_{m \notin \mathcal{Q}, m > k} P_m h_{u,m}$  and  $\sum_{n \in \mathcal{Q}} P_n h_{u,n}$  represent the intra-cluster, and inter-cluster interference, respectively.

### B. Problem Formulation

To maximize the total offloaded bits for the STAR-RIS-aided WPT-empowered MEC network with NOMA<sup>1</sup>, the following optimization problem is formulated, which requires to jointly optimize the resources allocated to energy transfer and uplink transmission tasks, i.e.,  $\mathcal{Z} = (\tau, \tau_k, P, P_k, \mathbf{v}_y^{\mathcal{X}})$ .

$$\max_{\mathcal{Z}} \sum_{1 \leq k \leq 2K} L_k(\tau_k, P_k, h_{u,k}) \quad (7a)$$

$$\text{s.t. } \eta P \tau h_{e,k} \geq P_k \tau_k, \quad \forall k \in \mathcal{K}_1, \mathcal{K}_2, \quad (7b)$$

$$\tau_k + \tau \leq T, \quad k \in \mathcal{K}_1, \mathcal{K}_2, \quad (7c)$$

$$|e^{j\theta_{y,n}^{\mathcal{X}}}| = 1, \quad \forall n \in \mathcal{N}, \quad \mathcal{X} = \{t, r\}, \quad \mathcal{Y} = \{e, u\} \quad (7d)$$

$$|\mathbf{v}_{y,n}^t|^2 + |\mathbf{v}_{y,n}^r|^2 = 1, \quad \forall n \in \mathcal{N}, \quad \mathcal{Y} = \{e, u\}, \quad (7e)$$

$$P \leq P_{\max}. \quad (7f)$$

where (7b) constrains the total consumed energy to total harvested energy for each user, whereas (7c) limits the uploading time. (7d -7e) model the phase and amplitude limitations of the STAR-RIS elements, whereas (7f) restricts the maximum transmit power at the AP.

### III. PROPOSED METHOD

We will first derive the optimal solution for  $P$  to simplify problem (7).

**Theorem 1.** *The optimal power of AP is  $P_{\max}$ .*

*Proof.* Assume the optimal power is  $P^*$ ,  $P^* < P_{\max}$ . The corresponding energy transfer time is  $\tau^*$ . For any given user, to harvest the same amount of energy, if we set the power to  $P_{\max}$  instead, we can reduce the transfer time from  $\tau^*$  to  $\frac{P^* \tau^*}{P_{\max}}$ . Accordingly, the time constraint for uplink transmission increases from  $T - \tau^*$  to  $T - \frac{P^* \tau^*}{P_{\max}}$ . With a loose time constraint for offloading, it is easy to verify that we could transmit more bits. This completes the proof.  $\square$

Under given optimal AP power, problem (7) is still non-convex, due to the non-convexity of constraints (7b) and (7d -7e). To address it, in the following, we decouple the original problem into three subproblems.

#### A. Subproblem 1: STAR-RIS Optimization during Energy Transfer Phase; $\mathbf{v}_e^{\mathcal{X}}$

Following the same argument in Theorem 1, it is clear that if we could maximize the channel response of the energy transfer phase for each user, the harvested energy is maximized, and so is the amount of the offloaded bit. Nevertheless, the phase shift optimization for different users often varies, and thus, it is often impossible to find a phase shift solution that meets all users' requirements. Aiming for an overall good performance,

<sup>1</sup>This is often called the computation rate maximization in the literature, since the total offloaded bits equal the offloading rate multiplied by the constant time  $T$  [14].

we propose to optimize  $\mathbf{v}_e^{\mathcal{X}}$  to maximize the sum channel gains of all users as follows:

$$\max_{\mathbf{v}_e^t, \mathbf{v}_e^r} \sum_{1 \leq k \leq 2K} |\mathbf{h}_{t,k}^H \text{diag}(\mathbf{v}_e^t) \mathbf{h}|^2 + |\mathbf{h}_{r,k}^H \text{diag}(\mathbf{v}_e^r) \mathbf{h}|^2 \quad (8a)$$

$$\text{s.t. } |e^{j\theta_{e,n}^{\mathcal{X}}}| = 1, \quad \forall n \in \mathcal{N}, \quad \mathcal{X} = \{t, r\}, \quad (8b)$$

$$|\mathbf{v}_{e,n}^t|^2 + |\mathbf{v}_{e,n}^r|^2 = 1, \quad \forall n \in \mathcal{N}. \quad (8c)$$

By defining  $\mathbf{h}_{t(k)}^H = \mathbf{h}_{t,k}^H \text{diag}(\mathbf{h})$  and  $\mathbf{h}_{r(k)}^H = \mathbf{h}_{r,k}^H \text{diag}(\mathbf{h})$ , (8) can be written as follows:

$$\max_{\mathbf{v}_e^t, \mathbf{v}_e^r} \sum_{1 \leq k \leq 2K} |\mathbf{h}_{t(k)}^H \mathbf{v}_e^t|^2 + |\mathbf{h}_{r(k)}^H \mathbf{v}_e^r|^2 \quad (9a)$$

$$\text{s.t. } (8b - 8c). \quad (9b)$$

Considering trace properties, we have the following semi-definite programming problem:

$$\max_{\Theta_e^t, \Theta_e^r} \text{Tr}(C_e^t \Theta_e^t) + \text{Tr}(C_e^r \Theta_e^r) \quad (10a)$$

$$\text{s.t. } \text{diag}(\Theta_e^t) + \text{diag}(\Theta_e^r) = \mathbf{1}^N, \quad \forall n \in \mathcal{N}, \quad (10b)$$

$$\Theta_e^{\mathcal{X}} \succeq 0, \quad \mathcal{X} = \{t, r\}, \quad (10c)$$

$$\text{Rank}(\Theta_e^{\mathcal{X}}) = 1, \quad \mathcal{X} = \{t, r\}. \quad (10d)$$

where  $C_e^{\mathcal{X}} = \sum_{k=1}^{2K} \mathbf{h}_{\mathcal{X}(k)} \mathbf{h}_{\mathcal{X}(k)}^H$  and  $\Theta_e^{\mathcal{X}} = \mathbf{v}_e^{\mathcal{X}} \mathbf{v}_e^{\mathcal{X}H}$ . After dropping the rank-1 constraint, problem (10) can be solved using the CVX toolbox in MATLAB [8], [15]. Then, Gaussian randomization could be utilized to obtain a rank-1 solution.

#### B. Subproblem 2: STAR-RIS Optimization during Uplink Transmission; $\mathbf{v}_u^{\mathcal{X}}$

Likewise,  $\mathbf{v}_u^{\mathcal{X}}$  can be heuristically obtained from the optimization problem below:

$$\max_{\mathbf{v}_u^t, \mathbf{v}_u^r} \sum_{1 \leq k \leq 2K} |\mathbf{g}^H \text{diag}(\mathbf{v}_u^t) \mathbf{g}_{t(I,k)}|^2 + |\mathbf{g}^H \text{diag}(\mathbf{v}_u^r) \mathbf{g}_{r,k}|^2 \quad (11a)$$

$$\text{s.t. } |e^{j\theta_{u,n}^{\mathcal{X}}}| = 1, \quad \forall n \in \mathcal{N}, \quad \mathcal{X} = \{t, r\}, \quad (11b)$$

$$|\mathbf{v}_{u,n}^t|^2 + |\mathbf{v}_{u,n}^r|^2 = 1, \quad \forall n \in \mathcal{N}. \quad (11c)$$

Similar to (8), it can be transformed into a semi-definite programming problem and solved using CVX in MATLAB, followed by Gaussian randomization.

Note that once the optimized values of  $\mathbf{v}_y^{\mathcal{X}}$  are obtained, they are fixed for the rest of the paper. On this basis, we will optimize the remaining variables, i.e.,  $\tau, \tau_k, P_k$ .

#### C. Subproblem 3: Time and Power Optimization; $\tau, \tau_k, P_k$

Under given  $(P^*, \mathbf{v}_y^{\mathcal{X}*}, \mathbf{v}_y^{\mathcal{X}*})$ , the main problem can be transformed into the following one:

$$\max_{\tau, \tau_k, P_k} \sum_{1 \leq k \leq 2K} L_k(\tau_k, P_k, h_{u,k}^*) \quad (12a)$$

$$\text{s.t. } \eta P_{\max} h_{e,k}^* \tau \geq P_k \tau_k, \quad \forall k \in \mathcal{K}_1, \mathcal{K}_2, \quad (12b)$$

$$\tau_k \leq T - \tau, \quad \forall k \in \mathcal{K}_1, \mathcal{K}_2. \quad (12c)$$

where  $h_{u,k}^*$  and  $h_{e,k}^*$  denote the corresponding channel gains of the uplink and energy transfer channels at user  $k$  after plugging the optimized value of  $\mathbf{v}_y^*$ . Therefore, both  $h_{u,k}^*$  and  $h_{e,k}^*$  are known constants.

For constraint (12c), it is easy to verify that equality holds for the optimal solution, i.e.,  $\tau_k^* = T - \tau$ . The reasons are twofold: 1) under any given consumed energy for transmission, increasing  $\tau_k$  leads to a larger  $L_k$ , since  $L_k$  is linear with  $\tau_k$  but follows a log function with power  $P_k$ ; 2) reducing  $P_k$  will yield less interference to other users as well, thus, boosts the overall performance. As a result, NOMA has been employed since  $\tau_k^* = T - \tau$ ,  $\forall k$ .

Now, we will optimize the remaining variables, i.e.,  $(\tau, P_k)$ , by looking into the following problem:

$$\max_{\tau, P_k} \sum_{1 \leq k \leq 2K} L_k(T - \tau, P_k, h_{u,k}^*) \quad (13a)$$

$$\text{s.t. } \eta P_{\max} h_{e,k}^* \tau \geq P_k(T - \tau), \quad \forall k \in \mathcal{K}_1, \mathcal{K}_2. \quad (13b)$$

Problem (13a) is still non-convex due to the existence of inter-cluster interference. Meanwhile, (13b) is non-convex due to the multiplication of  $P_k$  and  $\tau$ . Therefore, obtaining the optimal solution is still non-trivial. Here we propose an effective heuristic solution by simply assuming that each user uses all the harvested energy for uplink transmission. Therefore, we have the following equality:

$$P_k^* = \frac{\eta P_{\max} h_{e,k}^* \tau}{T - \tau}, \quad \forall k \in \mathcal{K}_1, \mathcal{K}_2. \quad (14)$$

Then, by leveraging the principles of telescopic series and substituting  $P_k^*$  into (13), the considered problem becomes:

$$\max_{\tau} B(T - \tau) \left( \log_2(g_1(\tau)) + \log_2(g_2(\tau)) \right) \quad (15)$$

where

$$g_1(\tau) = \frac{\sum_{k=1}^{2K} \eta P_{\max} h_{e,k}^* h_{u,k}^*}{\sum_{k=K+1}^{2K} \eta P_{\max} h_{e,k}^* h_{u,k}^* + \sigma^2 \left( \frac{T-\tau}{\tau} \right)}, \quad (16)$$

$$g_2(\tau) = \frac{\sum_{k=1}^{2K} \eta P_{\max} h_{e,k}^* h_{u,k}^*}{\sum_{k=1}^K \eta P_{\max} h_{e,k}^* h_{u,k}^* + \sigma^2 \left( \frac{T-\tau}{\tau} \right)}. \quad (17)$$

It can be easily verified that (15) is concave, and thus, the optimal  $\tau$  can be obtained using the bisection method.

The pseudo-code of the proposed solution is summarized in Algorithm 1.

The overall computational complexity is given by:

$$\mathcal{O} \left( 4N^3 \sqrt{(2N)} \log_2 \left( \frac{1}{\mu_1} \right) + \log_2 \left( \frac{T}{\mu} \right) \right). \quad (18)$$

where the first term is from SDR, while the second term is from the bisection method. Note that  $\mu$  and  $\mu_1$  denote the corresponding tolerance factors.

---

#### Algorithm 1 Proposed solution

---

- 1: **Input**  $\eta, K, P_{\max}, T, N, B, \epsilon, \mu$ , and  $\sigma^2$ .
  - 2: Obtain the optimal phase-shifts for all phases by solving (8), (11), employing CVX in MATLAB.
  - 3: Set  $\tau^L = \epsilon$ ;  $\tau^U = T - \epsilon$ ;  $\tau^M = \frac{\tau^L + \tau^U}{2}$ .
  - 4: **while**  $|\tau^L - \tau^U| > \mu$  **do**
  - 5:   Obtain uplink transmission time and power for all users (i.e  $\tau_k$  and  $P_k$ ) for the corresponding  $\tau^U$  and  $\tau^M$  from  $T - \tau$  and (14), respectively.
  - 6:   Compute  $L^U = \sum_{k=1}^{2K} L_k(\tau^U, P_k^U, h_{u,k}^*)$   
and  $L^M = \sum_{k=1}^{2K} L_k(\tau^M, P_k^M, h_{u,k}^*)$ .
  - 7:   Mean value =  $\frac{L^U - L^M}{\tau^U - \tau^M}$ .
  - 8:   **if** Mean value  $< 0$  **then**,  
     $\tau^U = \tau^M$ ;  $\tau^U = \frac{\tau^L + \tau^U}{2}$ ,
  - 9:   **else**  
     $\tau^L = \tau^M$ ;  $\tau^U = \frac{\tau^L + \tau^U}{2}$ ,
  - 10:   **end if**
  - 11: **end while**
  - 12: **Output**  
     $\mathcal{Z} = (\tau^M, T - \tau^M, P_{\max}, P_k^M, \mathbf{v}_y^*)$ .
- 

## IV. SIMULATION RESULTS

Numerical results are presented in this section to verify the effectiveness of the proposed scheme. The simulated system consists of two clusters, each with  $K = 4$  users distributed over two circles centered at (0 m, 10 m) and (10 m, 10 m) with a radius of 2.5 m. The AP is located at the origin, while the STAR-RIS is located at (5 m, 5 m) so that clusters A and B are covered by the reflection and transmission regions, respectively. The path loss between the STAR-RIS and AP or users is modeled as  $Cd^{-\beta}$ , where  $\beta = 3$ ,  $C = -30$  dB, and  $d$  are respectively the path loss component, the path loss at 1 m, and the distance between the STAR-RIS and AP/user. The channel bandwidth is 5 MHz, while the noise power is  $-100$  dBm. According to the above parameter settings, the proposed algorithm is run for 1000 iterations with an error tolerance of  $10^{-5}$  [14].

As for benchmark schemes, we first consider its OMA counterpart, represented by frequency division multiple access (FDMA) with equal bandwidth allocation. Although there exists no intra-cluster interference, inter-cluster interference still remains for OMA, which leads to similar problem formulation as in NOMA. Therefore, we apply the proposed solution to OMA as well. Moreover, under both NOMA and OMA, to show the effectiveness of phase optimization, we add the baseline, where the random phase shift is used to all elements of STAR-RIS. The optimization of the remaining variables follows the proposed scheme. Note that the case without STAR-RIS cannot be included, since the direct link between the AP and users is assumed blocked.

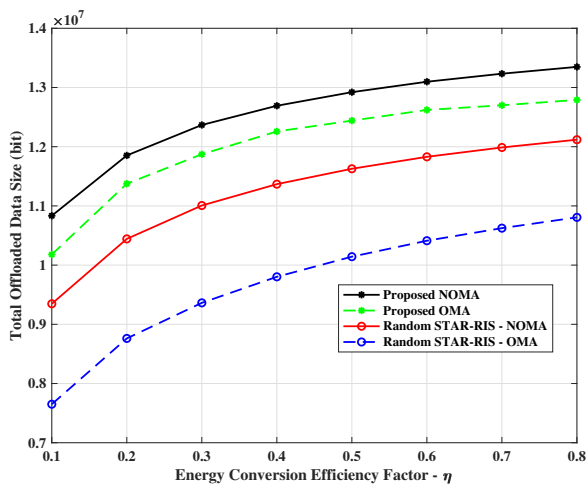


Figure 2: Total offloaded data size versus energy conversion efficiency for  $N = 50$ ,  $P_{\max} = 10$ , and  $T = 1$  s.

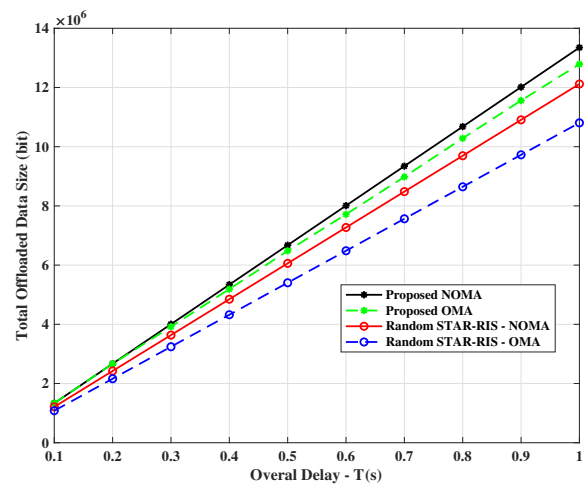


Figure 4: Total offloaded data size versus overall latency for  $N = 50$  and  $\eta = 0.8$ , and  $P_{\max} = 10$  W.

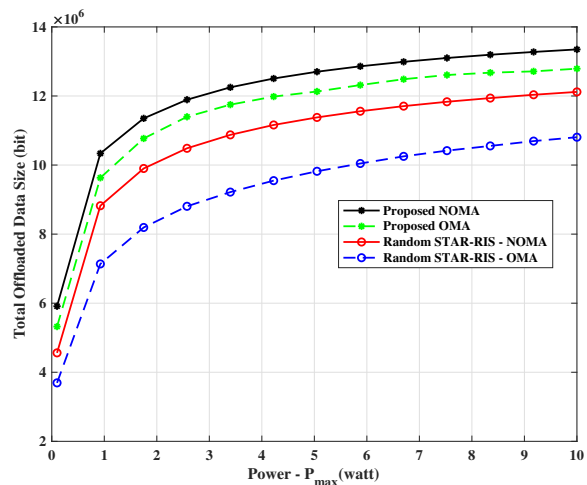


Figure 3: Total offloaded data size versus maximum power of AP for  $N = 50$ ,  $\eta = 0.8$ , and  $T = 1$  s.

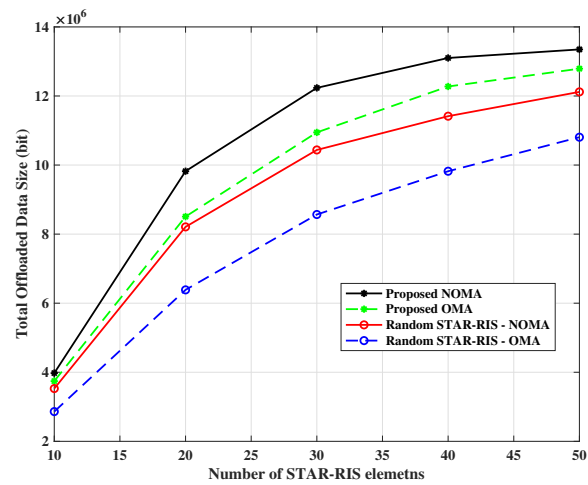


Figure 5: Total offloaded data size versus the number of RIS elements for  $P_{\max} = 10$  W,  $\eta = 0.8$ , and  $T = 1$  s.

Figure 2 shows how the total offloaded data size varies with the energy conversion factor. As expected, the performance of all the considered schemes grows with the energy conversion factor, owing to increased harvested energy. Among the considered schemes, it is clear that the proposed scheme under NOMA is the best, followed by proposed OMA, random STAR-RIS - NOMA, and finally, random STAR-RIS - OMA. The superiority of NOMA over OMA is evident, whereas the huge gap between the proposed scheme and random STAR-RIS under both NOMA and OMA validates the necessity of phase optimization.

Figure 3 plots the total offloaded data size versus the maximum power of the AP. Similar to Fig. 2, the overall

offloaded data size increases with  $P_{\max}$ , which matches the conclusion from Theorem 1. Meanwhile, the increase in data size with regard to  $P_{\max}$  slows down gradually, mainly due to the log function of transmission rate over transmission power. Once again, the proposed scheme under NOMA outperforms the baselines.

Figure 4 illustrates the total offloaded data size over the time constraint  $T$ . With a looser time constraint, more data can be offloaded for all the considered schemes. This is because a larger  $T$  can result in more harvested energy and more time for transmission. Moreover, the offloaded data size increases almost linearly with  $T$ , indicating that increasing  $T$  is more efficient in boosting system performance than increasing the

power.

Lastly, Fig. 5 presents how the total offloaded data size varies with the number of elements at the STAR-RIS. Not surprisingly, the system performance for all considered schemes is enhanced with the number of STAR-RIS elements, indicating more STAR-RIS elements is preferred. Meanwhile, similar to Figs 2-4, the proposed scheme under NOMA dominates the benchmarks.

## V. CONCLUSION

This paper maximized the overall offloaded data size in STAR-RIS aided WPT MEC networks by jointly optimizing the resources for transfer and uplink transmission, including the power, transfer/uplink phase beamforming of STAR-RIS, as well as transmission power and time slot allocation for WPT and task offloading. SDR was first employed to obtain the optimized amplitudes and phase shifts for STAR-RIS. On this basis, the bisection method was used for the time and power allocation during power transfer and uplink transmission. Presented numerical results demonstrated that the NOMA-based proposed scheme surpasses the existing benchmark schemes. Meanwhile, it was found that the system performance could be enhanced by increasing the number of STAR-RIS elements.

## REFERENCES

- [1] Z. Qadir, K. N. Le, N. Saeed, and H. S. Munawar, "Towards 6G internet of things: Recent advances, use cases, and open challenges," *ICT Express*, vol. 9, no. 3, pp. 296–312, 2023.
- [2] Z. Tong, J. Cai, J. Mei, K. Li, and K. Li, "Computation offloading for energy efficiency maximization of sustainable energy supply network in IoT," *IEEE Transactions on Sustainable Computing*, 2023.
- [3] S. Deshpande and N. Kulkarni, "Energy-efficient task offloading in edge computing with energy harvesting," *Sustainable Energy Solutions with Artificial Intelligence, Blockchain Technology, and Internet of Things*, pp. 145–156, 2024.
- [4] L. Shi, Y. Ye, X. Chu, and G. Lu, "Computation energy efficiency maximization for a NOMA-based WPT-MEC network," *IEEE Internet of Things Journal*, vol. 8, no. 13, pp. 10731–10744, 2021.
- [5] B. Liu, C. Liu, and M. Peng, "Resource allocation for energy-efficient mec in NOMA-enabled massive IoT networks," *IEEE Journal on Selected Areas in Communications*, vol. 39, no. 4, pp. 1015–1027, 2020.
- [6] M. Zeng, E. Bedeer, X. Li, Q.-V. Pham, O. A. Dobre, P. Fortier, and L. A. Rusch, "Irs-empowered wireless communications: State-of-the-art, key techniques, and open issues," in *6G Wireless: The Communication Paradigm Beyond 2030*. CRC Press, 2023, pp. 15–28.
- [7] X. Mu, Y. Liu, L. Guo, J. Lin, and R. Schober, "Simultaneously transmitting and reflecting STAR RIS aided wireless communications," *IEEE Transactions on Wireless Communications*, vol. 21, no. 5, pp. 3083–3098, 2021.
- [8] M. Asif, A. Ihsan, W. U. Khan, Z. Ali, S. Zhang, and S. X. Wu, "Energy-efficient beamforming and resource optimization for STAR-RIS enabled hybrid-NOMA 6G communications," *IEEE Transactions on Green Communications and Networking*, 2023.
- [9] Z. Liu, Z. Li, M. Wen, Y. Gong, and Y.-C. Wu, "STAR-RIS-aided mobile edge computing: Computation rate maximization with binary amplitude coefficients," *IEEE Transactions on Communications*, 2023.
- [10] S. Mao, N. Zhang, L. Liu, J. Wu, M. Dong, K. Ota, T. Liu, and D. Wu, "Computation rate maximization for intelligent reflecting surface enhanced wireless powered mobile edge computing networks," *IEEE Transactions on Vehicular Technology*, vol. 70, no. 10, pp. 10820–10831, 2021.
- [11] P. P. Perera, V. G. Warnasooriya, D. Kudathanthirige, and H. A. Suraweera, "Sum rate maximization in star-RIS assisted full-duplex communication systems," in *ICC 2022-IEEE International Conference on Communications*. IEEE, 2022, pp. 3281–3286.
- [12] M. Zeng, A. Yadav, O. A. Dobre, and H. V. Poor, "Energy-efficient power allocation for MIMO-NOMA with multiple users in a cluster," *IEEE Access*, vol. 6, pp. 5170–5181, 2018.
- [13] M. Alishahi, P. Fortier, W. Hao, X. Li, and M. Zeng, "Energy minimization for wireless-powered federated learning network with NOMA," *IEEE Wireless Communications Letters*, pp. 1–1, 2023.
- [14] S. Mao, L. Liu, N. Zhang, M. Dong, J. Zhao, J. Wu, and V. C. Leung, "Reconfigurable intelligent surface-assisted secure mobile edge computing networks," *IEEE Transactions on Vehicular Technology*, vol. 71, no. 6, pp. 6647–6660, 2022.
- [15] Z. Chu, Z. Zhu, F. Zhou, M. Zhang, and N. Al-Dhahir, "Intelligent reflecting surface assisted wireless powered sensor networks for internet of things," *IEEE Transactions on Communications*, vol. 69, no. 7, pp. 4877–4889, 2021.